Desalination and Water Treatment
www.deswater.com

doi: 10.5004/dwt.2017.20276

67 (2017) 284–291
March

Equilibrium and kinetic studies of methyl orange and Rhodamine B adsorption onto prepared activated carbon based on synthetic and agricultural wastes

Z. Chennouf-Abdellatif[a], B. Cheknane[a,*], F. Zermane[a], E.M. Gaigneaux[b], O. Mohammedi[a], N. Bouchenafa-Saib[a]

[a]*Laboratoire de Chimie Physique des Interfaces des Matériaux Appliquées a L'environnement, Faculty of Technology, University of Blida1, B.P. 270 Road Soumaa, Blida, Algeria, Tel. +213 55 487 804; Fax: +213 25 43 36 39; email: ocheknane@yahoo.fr*
[b]*Laboratory of Catalysis and Chemistry of Divided Materials, Institute of Condensed Matter and Nanoscience, University Catholique of Louvain, Croix du sud, 2 box L7.05.17 1348, Louvain-la-Neuve, Belgium*

Received 1 July 2016; Accepted 18 October 2016

ABSTRACT

The present study is focused on the valorization of a synthetic (tires) and agricultural (date pit) waste using a simple method in order to obtain an interesting activated carbon, which has been compared with commercial coal. Prepared active carbon is characterized by various techniques such as elemental analysis Brunauer, Emmett and Teller, elementary analysis, scanning electron microscopy (SEM), X-ray photoelectron spectroscopy (XPS), and temperature programmed desorption (TPD). Results of characterization of the two prepared carbons with chemical activation show clearly that a temperature of 550°C and particle diameter of 800 µm give interesting proprieties. The specific surface area reached 770 and 1,030 m^2/g, respectively, for the different active carbons obtained from tires and date pits. The ratio of carbon in the two prepared activated carbons reached 83% and 93%, respectively for the elementary analysis and surface chemical composition, and the analysis by TPD shows the formation of different functional groups (as radicals, carbonyl groups, and aromatic ethylinique). In order to evaluate the efficiency of these adsorbents, we selected an anionic dye (orange methyl) as a pollutant. Kinetic results show that the adsorption equilibrium is reached at around 60 min with an adsorbed amount of 21.42 and 38.83 mg/g for the tire activated carbon (TAC) and the date pits activated carbon (DPAC) , respectively. The different isotherms were well fitting by the Freundlich model.

Keywords: Activated carbon; Tires; Date pits; Dye adsorption

1. Introduction

Nowadays many industries, particularly those in the textile, reject in rivers colored by-products. These organic compounds have a high toxicity, which can lead to serious environmental problems. In an optical decontamination of these waters, activated carbon, highly developed porous texture material remains by far the adsorbent of choice in environmental clean due to its large capacity and its adsorption selectivity [1]. Activated carbon is widely used for treatment wastewater in many industries. According to the literature as synthetic adsorbents showed good potential for the elimination of dyes in aqueous solutions [2–7]. The dyes are widely used in the printing, food, cosmetic and clinical, but in particular in the textile industries for their chemical stability and ease of synthesis and variety of colors. However, these dyes are causing pollution when released into the environment [8,9]. Studies have shown that many azo dyes are toxic and mutagenic and biological treatment of these dyes appears to be of major scientific interest [10,11].

---

* Corresponding author.

1944-3994/1944-3986

Numerous studies have been published in the literature on the toxicity of chemicals [8,12–14], in particular, the methyl orange (MO) and Rhodamine B (RhB) are two important dyes that are widely used in textile industry.

The increasing demand in adsorbent materials drives research toward the production of activated carbons from unconventional materials, such as synthetic and agricultural waste.

Several studies have shown the production and characterization of activated carbons from a wide range of materials of different origins [16–24]. With a unique aim of developing these activated carbon materials, we used like precursors the date pits coming from the Algerian south (Deglet Nour) and tire scrap (worn tire of the same car [Michelin Primacy HP]).

Generally, the preparation of activated carbon can be divided into three categories such us: (1) chemical activation with H_3PO_4 [25], (2) physical activation with CO_2 and (3) a combined method using both CO_2 and H_3PO_4.

It is known that the chemical activation is often preferred [26] due to several economic and structural reasons. The most important agents are used phosphoric acid [27], zinc chloride [28–30] and alkali metal hydroxides [31]. Phosphoric acid has been particularly used for several decades [32,33] to prepare activated carbon with large specific surfaces [34], and its method of preparation is widely described in the literature [35–37]. It has also been demonstrated that the distribution of the porosity of the activated carbon in the H_3PO_4 is heterogeneous.

In this study, we focused on the valorization aspect. In this context, we used the waste tires and an agricultural waste (date pits) as precursors of activated carbons. Selected diameter is between 800 and 2,500 µm, and the temperature range is between 400°C and 600°C. These materials include various applications such as the purification of fluids by adsorption, storage of gas. They are also used in heterogeneous catalysis as carriers of the active phase. These adsorbents were evaluated for the treatment of industrial textile water by adsorption process.

2. Methods and materials

Waste tires used in this study were originally from tires of the same car (Michelin Primacy HP). The agricultural waste the date pits (Deglet Nour) come from south Algeria (collected in 2010). The chemical agents used are H_3PO_4 (85%), CO_2 and H_3PO_4/CO_2 [38].

The two starting materials were washed with distilled water and dried in an oven at 105°C for 24 h. They are then cut and ground and sieved to retain the granulometric fraction with diameter between 800 and 2,000 µm.

2.1. Chemical pretreatment and preparation of activated carbon

2.1.1. Using phosphoric acid

Method consists to introducing in a reactor, a mixture containing a fixed mass of the chosen granulometric fraction with 2 ml of H_3PO_4 (85%) per gram as proposed in [38]. The mixture was refluxed at 85°C during a time of 2 h then carbonized in a quartz tubular reactor of a diameter of 3 cm at 500°C under a flow of 20 l/h of nitrogen. In order to eliminate the excess of H_3PO_4, the prepared carbon has been washed with water in a Soxhlet extractor several times until a neutral pH was reached (20 cycles). Finally, the prepared sample was dried at 110°C in an oven [39].

2.1.2. Using carbon dioxide

In this activation, there are two steps: the first one is the carbonization and the second one is activation of the raw material. Carbonization is the thermal decomposition at high temperature under inert gas (we use generally the nitrogen); the activation is carried out in a chamber preheated to 600°C under controlled flow of oxidant gases (such as the carbon dioxide). Temperature is maintained for a period of 1 h to obtain a dry residue. Obtained material is washed with distilled water under reflux until neutralization of the rinsing water.

2.1.3. Using carbon dioxide and phosphoric acid (H_3PO_4/CO_2)

In this part of activation, the particles of the selected diameter are first impregnated with 2 ml/g of H_3PO_4 (chemical activation), and then subjected to a temperature rise of 10°C/min up to different temperatures (500°C–850°C) under a flow of 20 L/h of nitrogen. When the temperature is reached, the nitrogen is replaced by CO_2 (physical activation), and the activation persists during 1 h.

2.2. Physicochemical characterization of activated carbon

Prepared coals by the various methods such as: physical activation realized with 850°C for the tire and date pits, respectively, tire activated carbon 3 (TAC3) and date pit activated carbon 3 (DPAC3), chemical activation with the phosphoric acid (TAC1), (DPAC1) and finally by the method combined (TAC2), (DPAC2) were characterized with several methods, particularly the elementary surface composition, which is carried out by the X-ray photoelectron spectroscopy (XPS).The spectra were acquired at a pressure of 10_6 Pa with an Al X-ray source at 8 eV.

The surface area were determined from nitrogen adsorption isotherms measured at liquid nitrogen temperature using an ASAP 2010 sorptometer (Micromeritics) equipped by software for accessing to the specific surface (Asp) according to classic Brunauer, Emmett and Teller (BET) [40]. The total pore volume was estimated from the adsorbed amount at a relative pressure between 0.9850 and 0.9990. The micropore volume is determined by the Dubinin–Astakhov model [41].

In order to detect the differences in morphology of prepared coals, photographs were taken using a microscope LEO 982 operative GEMINI under an accelerated tension of 1 eV and a current of 70 µA.

The thermal technique of programmed desorption is based on the amount of desorbed CO and CO_2 according to the temperature, which was detected by spectroscopy of masses. The sample is heated until a temperature of 1,000°C under a helium current of 60 cm^3/min with a rise of temperature of 20°C/min. A thermocouple is related to a controller of the temperature.

2.3. Application to the adsorption

In the adsorption field, it is known that the determination of the contact time to reach adsorption equilibrium represents the most significant step. In our case, we studied the kinetic adsorption of MO and RhB adsorption onto the different prepared activated carbon (DPAC and TAC), and the obtained results were compared with commercial activated carbon (CAC).

Adsorption kinetic experiments of the selected adsorbents in a static reactor were carried out in a series of reagent bottles at constant temperature of 25°C, by mixing 0.05 g of activated carbon in 50 mL of dye solution of 50 mg L^{-1} at fixed pH of 6. The solutions were stirred for 6 h using a type of shaker (Edmund Buhler GmbH SM - 30) and then filtered. Lagergren's pseudo-first-order model, Eq. (1), and Ho's pseudo-second-order model, Eq. (2), were applied to the data:

$$q = q_e(1 - e^{-k_1 t}) \tag{1}$$

$$q = \frac{q_e^2 k_2 t}{1 + q_e k_2 t} \tag{2}$$

where q_e and q (mg g^{-1}) are the amount of dye adsorbed at equilibrium and time t (min); k_1 (min^{-1}) is the pseudo-first-order rate constant; and k_2 (g mg^{-1}min^{-1}) is the pseudo-second-order rate constant.

The adsorption isotherms are important in determining the maximum adsorption capacities and the design of new adsorbents. In our case, isotherm studies were conducted by shaking different quantities of sorbent (from 0.01 to 0.1 g) with 50 mL of the dye solution (50 mg/L) at pH 6.

There are many theoretical models that have been developed to describe the adsorption isotherms. In our study, we used the most widely used isotherm models of Langmuir and Freundlich given by Eqs. (3) and (4), respectively:

$$q_e = q_m \frac{k_L C_e}{1 + k_L C_e} \tag{3}$$

$$q_e = K_F C_e^{1/n} \tag{4}$$

3. Results and discussion

3.1. Characterization results

The knowledge of the characteristics of the activated carbon is necessary to contribute to the comprehension of many phenomena like adsorption, desorption, the exchange or others. Tables 1 and 2 represent the different results of the specific surface area obtained by the three methods.

The chemical activation develops larger areas with a maximum of 770 m$_2$/g at 550°C for the tire (800 μm), at high temperature, the surface decreases. For 2 mm diameter particles, activation with the same chemical agent corresponds to significantly greater surface areas with a maximum of 654 m^2/g.

We can observe also that the surface does not exceed 400 m^2/g at optimum activation temperatures (550°C) for the combined method and physical method; this reduction is probably due to the saturation of activated sites by CO$_2$.

Concerning the date of pits (agricultural waste), which are activated by the chemical method, we obtained an optimum specific surface area of 1,030 and 540 m^2/g at 550°C, respectively, for particles diameters of 800 μm and 2 mm. However, the activation by the combined method decreases the surfaces areas to 820 and 540 m^2/g, respectively, for the same type of diameter. For the physical activation, the specific surface area decreases greatly (123 and 116 m^2/g).

The decrease in the volume of microporous carbons prepared by the three activation methods shows that these coals are rather mesoporous nature, which justifies the high values of specific surfaces. These results show also that the values of mesoporous volumes of the two diameters for the date pits and the tire are 0.519–0.522 cm^3/g and 1.103–0.430 cm^3/g, respectively. We can note that the specific surface profile follows exactly the behavior of the total pore volume of activated carbon.

The XPS analysis of the two coals at particles diameter of 800 μm obtained by chemical activation and the combined method at 550°C under nitrogen flow show the presence of carbon (C) and oxygen (O) (see Figs. 1(a)–(d)).

Results of elementary analysis and the surface chemical composition of prepared coals, given as atomic percentages, are represented in Table 3. We can notice that the essence of the carbonized or activated matter is carbon. The high percentage of this element (around 93%) explains a good pyrolysis of our material (waste synthetic and agricultural) and interprets a good enrichment of the precursor of carbon. This later develops new functional groups.

Results of the elementary analysis also show that the percentage of carbon is important, which exceeds the 81%; on the other hand, we can see clearly the ratio of hydrogen is lower than 1.2% for the four prepared activated carbon.

The DPAC obtained by combined method and chemical activation for TAC2 and DPAC1 show the presence of the phosphorus element (0.86% and 0.58%, respectively, Figs. 1(a) and 1(b)). This element can come only from the phosphoric acid used for the activation and could not be eliminated by simple washing [22]. For the same element on the TAC1 and DPAC2 materials, the ratio is much weaker (0.26 and 0.42, respectively, Figs. 1(c) and 1(d)).

On the spectrum (Figs. 1(a)–(d)), a high peaks of carbon are observed explaining the presence of groups CO, C=O and OC=O. The presence of these groups on the materials surface reveals a good oxidation of our materials by carbonization with carbonic gas or chemically (phosphoric acid) (see Figs. 1(a)–(d)).

Globally, it is noted that there is occurrence of two distinct peaks of CO and CO$_2$ with increasing temperature. CO occurs at high temperatures (around 700°C) characteristic of the high acidity (OH, COOH, CO), except for the Fig. 2(b) having two peaks at 700°C and 650°C. CO$_2$ appears at low temperatures of around 150°C, except in Fig. 2(d), which has a large peak at a temperature of 250°C.

The observations under the electron microscope with sweeping at 550°C for the different activated carbons chemically activated with phosphoric acid show that the activated carbon (TAC1) has a very developed porosity over the entire surface with some heterogeneity. For activated carbon (DPAC1), the external morphology has more or less homogeneous cavities on

Table 1
Results of the specific surface area and porous volume of tire activated carbon

Nature of coal	Agent of activation at 550°C	Granulometry	Asp (BET) (m^2/g)	Vol$_{ptot}$ (cm^3/g)	Vol$_{\mu p}$ (cm^3/g)	Vol$_{\text{més}}$ (cm^3/g)
TAC1	H_3PO_4	800 µm	**770**	0.544	0.018	0.519
		2 mm	**654**	0.553	0.031	0.522
TAC2	CO_2/H_3PO_4	800 µm	**390**	0.220	0.030	0.182
		2 mm	**271**	0.268	0.011	0.257
TAC3	CO_2	800 µm	**354**	0.350	0.002	0.348
		2 mm	**200**	0.010	0.007	0.003

Table 2
Results of the specific surface area and porous volume of date pit activated carbon

Nature of coal	Agent of activation at 550°C	Granulometry	Asp (BET) (m^2/g)	Vol$_{ptot}$ (cm^3/g)	Vol$_{\mu p}$ (cm^3/g)	Vol$_{\text{més}}$ (cm^3/g)
DPAC1	H_3PO_4	800 µm	**1030**	1.246	0.040	1.103
		2 mm	**540**	0.520	0.023	0.430
DPAC2	CO_2/H_3PO_4	800 µm	**820**	0.720	0.470	0.650
		2 mm	**540**	0.816	0.078	0.731
DPAC3	CO_2	800 µm	**123**	–	0.034	–
		2 mm	**116**	–	0.043	–

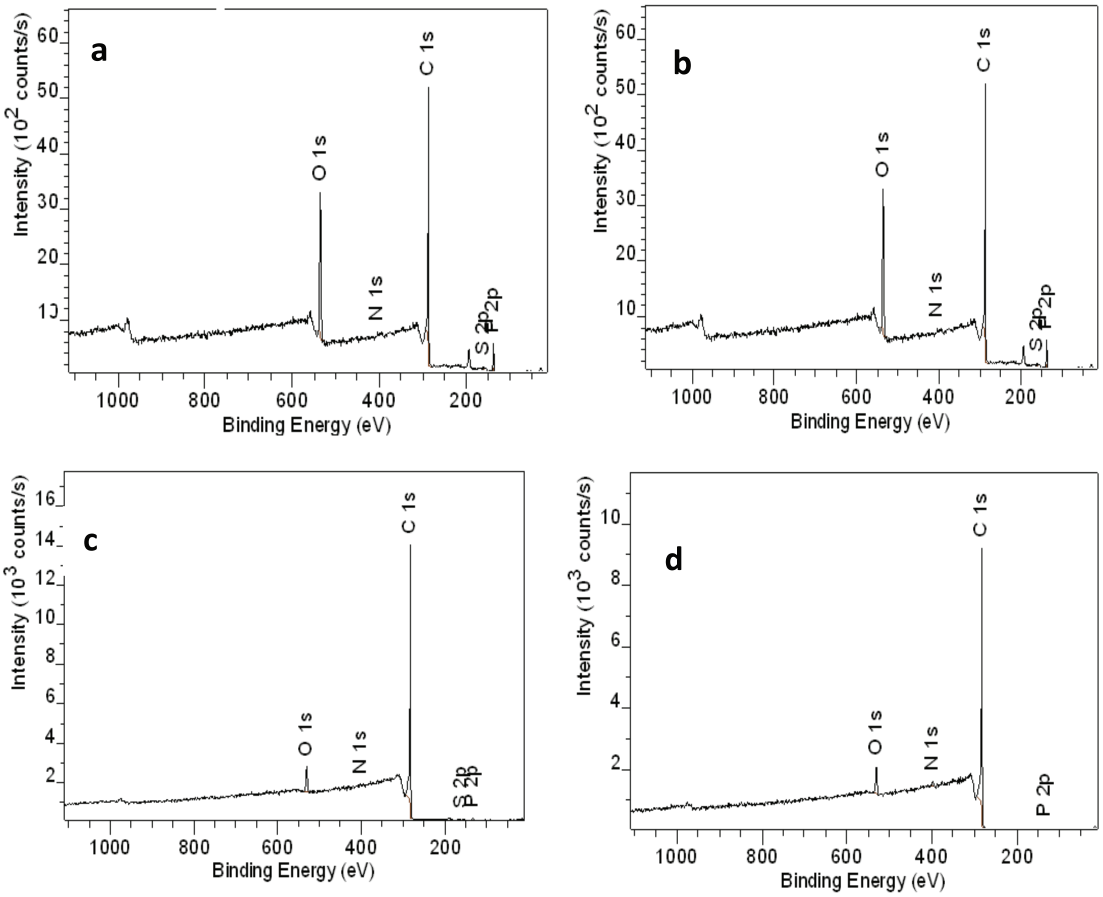

Fig. 1. XPS spectrum of activated carbons prepared by the combined and chemical activation for: (a) TAC2, (b) DPAC1, (c) TAC1, and (d) DPAC2, $T = 550°C$, $d = 800$ µm.

Table 3
Results of elementary analysis and chemical composition of surface by XPS for the prepared activated carbon

550°C	Elementary analyses (%)				Chemical composition of surface (%)			
	C	H	O	S	C	O	P	S
TAC1	83.64	0.24	16.12	1.72	91.60	7.12	0.26	0.42
TAC2	89.49	0.41	10.10	0.00	93.43	4.91	0.86	0.27
DPAC1	81.24	1.20	17.56	1.00	90.66	6.50	0.58	–
DPAC2	89.29	0.57	10.14	1.13	92.37	5.68	0.42	0.04

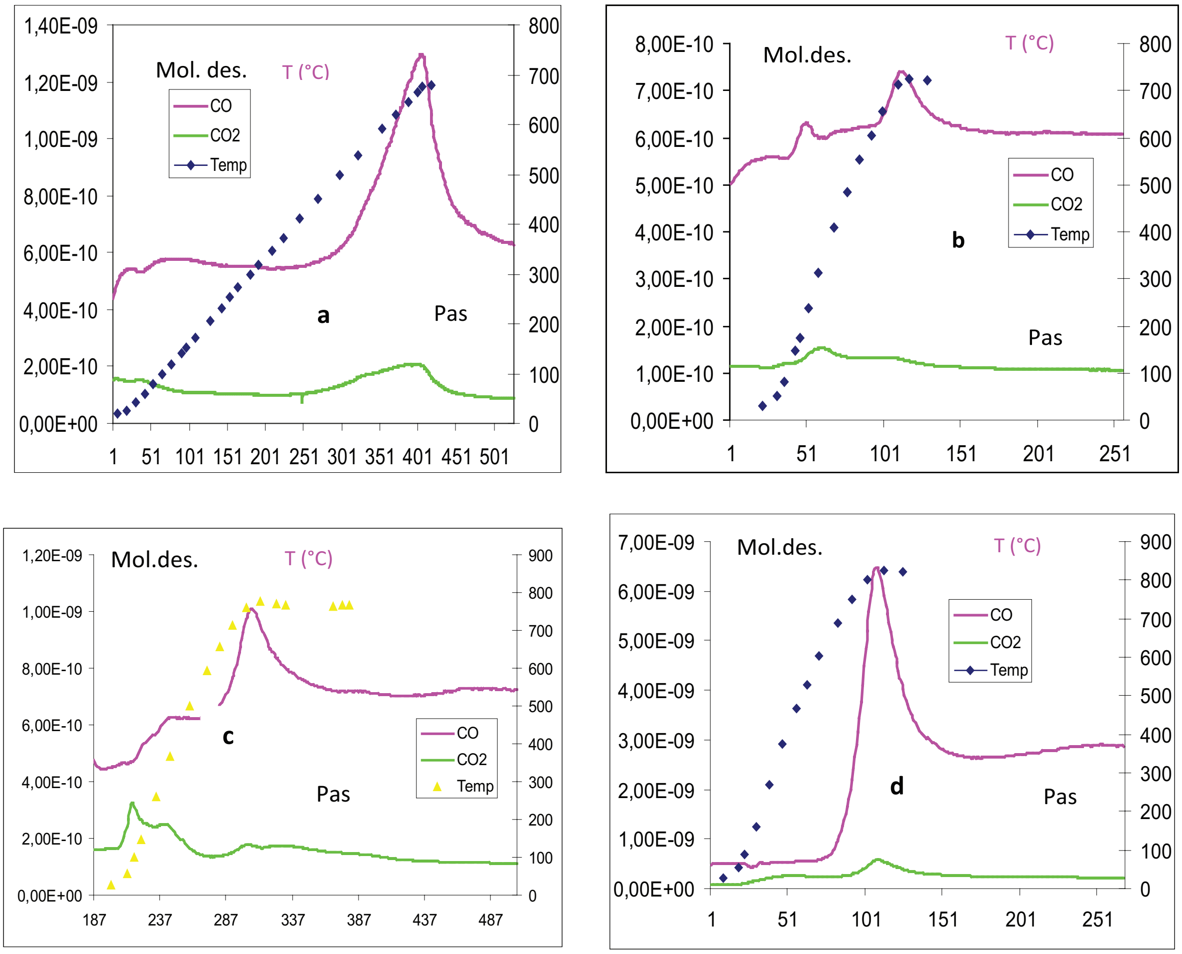

Fig. 2. Thermal desorption diagram for CO, CO_2 for two active carbon at 550°C: (a) TAC1, (b) TAC2, (c) DPAC1, and (d) DPAC2.

all surfaces. These cavities are probably obtained by evaporation of the chemical agent when activating leaving empty cavities.

4. Application to adsorption

Kinetic adsorption curves of the MO and RhB onto the two prepared activated carbon (TAC and DPAC) compared with the CAC are presented as adsorbed amount vs. time ($Q = f(t)$). According to Fig. 3(a), we can see clearly that for all kinetic curves the amount adsorbed increases with stirring time and reaches maximum values of 49, 48 and 46 mg.g^{-1} for CAC, DPAC and TAC, respectively. For RhB (Fig. 3(b)), the adsorbed amounts are 45, 44 and 41, respectively, for the CAC, CAP and DPAC. From these results, we can conclude that the adsorption of MO is more important than that of RhB to activated carbons prepared namely CAN, CAP and the CAC.

We can see also that the time of pseudo-equilibrium for the three kinds of activated carbon was faster around 5 min, which indicated the efficiency of prepared activated carbon.

Modeling results show clearly (Table 4) that the pseudo-second-order model properly depicts the adsorption process in agreement with the results of Cheknane et al. [42] for the adsorption of Basic Yellow 28 and malachite green onto granular pillared clay. The prepared activated carbon have a significantly higher rate constant ($K_1 > 0.011$ min^{-1}) than CAC

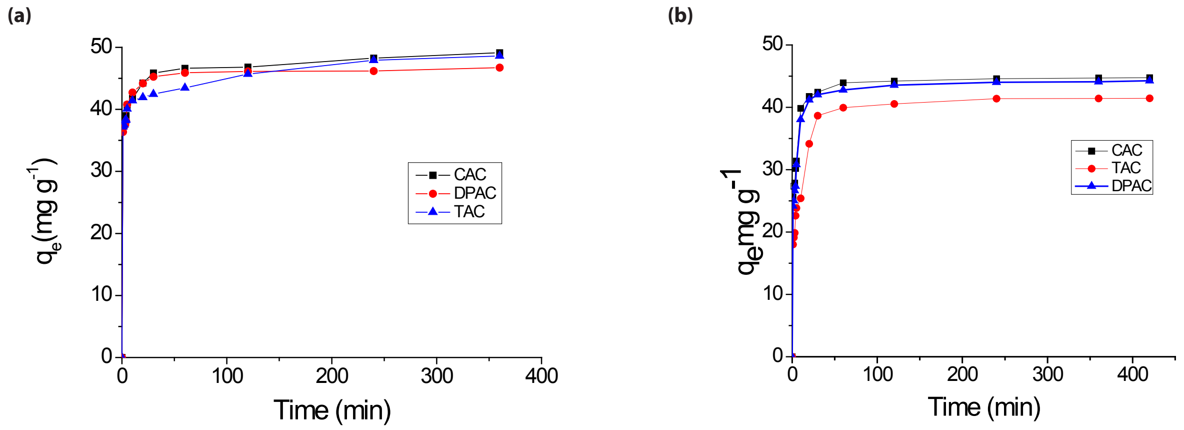

Fig. 3. Kinetic adsorption of orange methyl (MO) and Rhodamine B onto CAC, DPAC, and TAC.

Table 4
Kinetic adsorption constant from pseudo-first-order and pseudo-second-order model

		Pseudo-first-order model		Pseudo-second-order model	
		K_1 (min^{-1})	R^2	K_2 (g mg^{-1} min^{-1})	R^2
CAC	MO	0.0069	0.87	0.0055	0.99
	RhB	0.0450	0.71	0.0014	0.99
DPAC	MO	0.251	0.95	0.011	0.99
	RhB	0.317	0.94	0.015	0.99
TAC	MO	0.0102	0.78	0.0086	0.99
	RhB	0.0102	0.79	0.0086	0.99

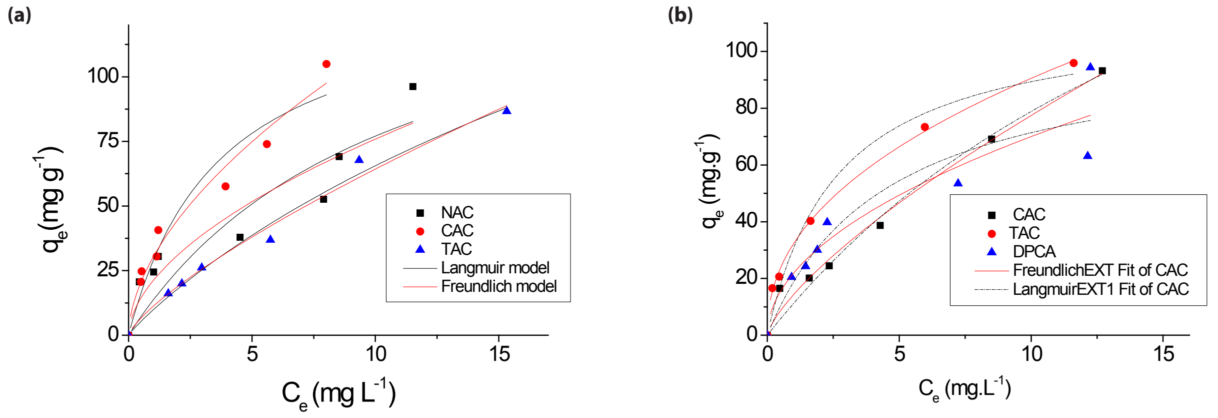

Fig. 4. Adsorption isotherms of orange methyl and Rhodamine B onto CAC, DPAC, and TAC.

(K_1 = 5.5.10–3) and (K_1 > 0.0014 min^{-1}) for RhB, this is can be explained by the structural proprieties of prepared activated carbon.

The adsorption isotherms can be shown by Fig. 4, which presents $Q = f(C_e)$. From this figure and for all used adsorbents, we can see that the evolution of the adsorption capacity Q_e equilibrium depending on the residual concentration of dye and the nature of activated carbon. The maximum amount of adsorption decreases in the following order: for MO: QCAC = 104 mg g^{-1}, QTAC = 96 mg g^{-1} and QDPAC = 86 mg g^{-1}, and for RhB: QCAC = 93 mg g^{-1}, QTAC = 96 mg g^{-1} and QDPAC = 94 mg g^{-1}.

On the other hand, we note that different isotherms obtained for the three adsorbents the types S curves according to Gilles classification. Which indicates that the adsorbed molecules promote the subsequent adsorption

Table 5
Freundlich parameter of used adsorbents

		K_f ($mg^{1-1/n}$ $L^{1/n}$ g^{-1})	n	R^2
CAC	MO	30.280	0.560	0.960
	RhB	14.330	0.732	0.982
DTAC	MO	21.150	0.554	0.860
	RhB	21.931	0.504	0.861
TAC	MO	11.190	0.758	0.998
	RhB	32.343	0.447	0.998

to other molecules (cooperative adsorption due to attractions between molecules of the solute by van der Waals forces)? Modeling results of obtained isotherms (Table 5) shows that the Freundlich model describe well our system, with values of $n < 1$ note the favorable adsorption and Freundlich equilibrium constant ($K_f > 12$ $mg^{1-1/n}$ $L^{1/n}$ g^{-1}) for all adsorbents.

The results of the maximum adsorption values (Q_{max}) of activated carbon prepared from synthetic waste (tires) and agricultural waste (date pits) show great potential as an adsorbent for the MO.

5. Conclusion

This present study was carried out in two steps: the first one was focused on the preparation of activated carbons from synthetic waste (tires) and agricultural waste (date pits), and the second step is basically concerned with the characterization of prepared adsorbents. The size does not affect the texture of activated carbons prepared whatever the nature of the precursor used. The date stones develop surrounding the large specific surface 1,030 m^2/g; particularly for the chemical method, tires develop a lesser porosity (770 m^2/g) by the same method. Finally, these interesting textural properties make activated carbon produced from agricultural waste and synthetic high potential as adsorbents of pollutants or as catalyst supports. Application of this new generation in the adsorption of MO and RhB shows that great potential as an adsorbent for MO and RhB compare with other adsorbents with ($q_{max} > 86$ mg g^{-1}).

References

[1] N. Bouchemal, Z. Merzougui, F. Addoun, Adsorption in aqueous media of two activated carbon dyes based on date pits, J. Soc. Alger. Chim., 21 (2011) 1–14.

[2] G. Sharma, M. Naushad, D. Pathania, A. Mittal, G.E. El-Desoky, Modification of *Hibiscus cannabinus* fiber by graft copolymerization: application for dye removal, Desal. Wat. Treat., 54 (2015) 3114–3121.

[3] M. Naushad, A. Mittal, M. Rathore, V. Gupta. Ion-exchange kinetic studies for Cd(II), Co(II), Cu(II), and Pb(II) metal ions over a composite cation exchanger, Desal. Wat. Treat., 54 (2015) 2883–2890.

[4] A. Mittal, R. Ahmed, I. Hasan, Iron oxide-impregnated dextrin nanocomposite: synthesis and its application for the biosorption of Cr(VI) ions from aqueous solution, Desal. Wat. Treat., 57 (2016) 15133–15145.

[5] A. Mittal, R. Ahmed, I. Hasan, Poly(methylmethacrylate)-grafted alginate/Fe_3O_4 nanocomposite: synthesis and its application for the removal of heavy metal ions, Desal. Wat. Treat., 57 (2016) 19820–19833.

[6] A. Mittal, M. Naushad, G. Sharma, Z.A. Alothman, S.M. Wabaidur, M. Alam, Fabrication of MWCNTs/ThO_2 nanocomposite and its adsorption behavior for the removal of Pb(II) metal from aqueous medium, Desal. Wat. Treat., 57 (2016) 21863–21869.

[7] A. Mittal, J. Mittal, Hen Feather: A Remarkable Adsorbent for Dye Removal, Green Chemistry for Dyes Removal from Wastewater: Research Trends and Applications, Chapter 11, S.K. Sharma, Ed., Scrivener Publishing LLC, USA, 2015, pp. 209–457.

[8] H. Ben Mansour, O. Boughzala, D. Dridi, D. Barillier, L. Chekir-Ghedira, R. Mosrati, Textiles dyes as a source of wastewater contamination: screening of the toxicity and treatment methods, J. Water Sci., 24 (2011) 209–238.

[9] A. Mittal, Retrospection of Bhopal gas tragedy, Toxicol. Environ. Chem., 98 (2016) 1079–1083.

[10] H. Ben Mansour, R. Mosrati, D. Corroler, D. Bariller, K. Ghedira, D. Bariller, L. Chekir-Ghedira, In vitro study of DNA damage induced by acid orange 52 and its biodegradation derivatives, Environ. Toxicol. Chem., 28 (2009) 489–495.

[11] P. Quillardet, M. Hofnung, The SOS chromotest: a review, Mutat. Res.-Rev. Genet., (1993) 235–279.

[12] H. Trabelsi, Study of the Degradation and Toxicity of Dyes by Ozonation and Photocatlysis, phD thesis, Chemistry, University de Monastir, 2014.

[13] H. Trabelsi, M. Khadhraoui, O. Hentati, M. Ksibi, Titanium dioxide mediated photo-degradation of methyl orange by ultraviolet light, Toxicol. Environ. Chem., 95 (2013) 543–558.

[14] R. Garnier, Archives of Occupational Diseases and the Environment, Elsevier Masson SAS, France, 76 (2015) 609–610.

[15] A. Ayar, O. Gezici, M. Küçükosmanoğlu, Adsorptive removal of methylene blue and methyl orange from aqueous media by carboxylated diaminoethane sporopollenin: on the usability of an aminocarboxilic acid functionality-bearing solid-stationary phase in column techniques, J. Hazard. Mater., 146 (2007) 186–193.

[16] V.M. Ospina-Guarín, R. Buitrago-Sierra, D.P. López-López, Preparation and characterization of activated carbon from castor de-oiled cake, Tecno Lógicas, 32 (2014) 75–84.

[17] A.M.M. Vergas, A.L. Gazetta, C.A. Garcia, J.C.G. Moraes, Preparation and characterization of activated carbon from a new raw lignocellulosic material: flamboyant (*Delonix regia*) pods, J. Environ. Manage., 92 (2011) 178–184.

[18] M. Trachi, N. Bourfis, S. Benamara, H. Gougam, Preparation and characterization of an activated carbon from the almond shell bitter (*Prunus amygdalus*), Biotechnology, Agronomy, Society and Environment, 18 (2014) 492–502.

[19] Y.X. Wang, H.H. Ngo, W.S. Guo, Preparation of a specific bamboo based activated carbon and its application for ciprofloxacin removal, Sci. Total Environ., 533 (2015) 32–39.

[20] J.M.V. Nabais, C. Laginhas, M.M.L.R. Carrott, P.J.M. Carrott, J.E. Crespo Amoros, A.V. Nadal Gisbert, Surface and porous characterisation of activated carbons made from a novel biomass precursor, the esparto grass, Appl. Surf. Sci., 265 (2013) 919–924.

[21] D.A.S. Maia, K. Sapag, J.P. Toso, R.H. Lopez, D.C.S. Azevedo, C.L. Cavalcante Jr., G. Zgrablich, Characterization of activated carbon from peach stones through the mixed geometry model, Microporous Mesoporous Mater., 134 (2010) 181–188.

[22] H. Demiral, I. Demiral, B. Karabacakoglu, F. Tumsek, Production of activated carbon from olive bagasse by physical activation, Chem. Eng. Res. Des., 89 (2011) 206–213.

[23] D. Mohan, A. Sarswat, V.K. Singh, M. Alexandre-Franco, C.U. Pittman Jr., Development of magnetic activated carbon from almond shells for trinitrophenol removal from water, Chem. Eng. J., 172 (2011) 1111–1125.

[24] A.M.M. Vargas, A.L. Cazetta, C.A. Garcia, J.C.G. Moraes, E. Nogami, E.M. Lenzi, W.F. Costa, V.C. Almeida, Preparation and characterization of activated carbon from a new raw

lignocellulosic material: flamboyant (*Delonix regia*) pods, J. Environ. Manage., 92 (2011) 178–184.

[25] H. Deng, L. Yang, G. Tao, J. Dai, Preparation and characterization of activated carbon from cotton stalk by microwave assisted chemical activation – application in methylene blue adsorption from aqueous solution, J. Hazard. Mater., 166 (2009) 1514–1521.

[26] Q.S. Liu, T. Zheng, P. Wang, L. Guo, Preparation and characterization of activated carbon from bamboo by microwave-induced phosphoric acid activation, Ind. Crops Prod., 31 (2010) 233–323.

[27] N.V. Sych, S.I. Trofymenko, O.I. Poddubnaya, M.M. Tsyba, V.I. Sapsay, D.O. Klymchuk, A.M. Puziy, Porous structure and surface chemistry of phosphoric acid activated carbon from corncob, Appl. Surf. Sci., 261 (2012) 75–82.

[28] Y. Gherairi, A. Amrane, Y. Touil, Comparative study of the addition effect of activated carbon obtained from date stones on the biological filtration efficiency using sand dune bed, Energy Procedia, 36 (2013) 1175–1183.

[29] S. Uçar, M. Erdem, T. Tay, S. Karagoz, Preparation and characterization of activated carbon produced from pomegranate seeds by $ZnCl_2$ activation, Appl. Surf. Sci., 255 (2009) 8890–8896.

[30] S. Yorgun, N. Vural, H. Demiral, Preparation of high-surface area activated carbons from Paulownia wood by $ZnCl_2$ activation, Microporous Mesoporous Mater., 122 (2009) 189–194.

[31] S.B. Girgis, A.N.A. El-Hendawy, Porosity development in activated carbons obtained from date pits under chemical activation with phosphoric acid, Microporous Mesoporous Mater., 52 (2002)105–117.

[32] O.A. Olafadehan, O.W. Jinadu, L. Salami, O.T. Popoola, Treatment of brewery wastewater effluent using activated carbon prepared from coconut shell, Inter. J. Appl. Sci. Tech., 2 (2012) 165–178.

[33] A. Cobb, M. Warms, E.P. Maurer, Low-tech coconut shell activated charcoal production, Int. J. Serv. Learn. Eng., 7 (2012) 93–104.

[34] L. Feng, J. Zheng, H. Yang, Y. Guo, W. Li, X. Li, Preparation and characterization of polyethylene glycol/active carbon composites as shape-stabilized phase change materials, Sol. Energy Mater. Sol. Cells, 95 (2011) 644–650.

[35] Y. Nakagawa, M. Molina-Sabio, F. Rodrıguez-reinoso, Modification of the porous structure along the preparation of activated carbon monoliths with H_3PO_4 and $ZnCl_2$, Microporous Mesoporous Mater., 103 (2007) 29–34.

[36] M. Molina-Sabio, C. Almansa, F. Rodrıguez-Reinoso, Phosphoric acid activated carbon discs for methane adsorption, Carbon, 41 (2003) 2113–2119.

[37] H. Hadoun, Z. Sadaoui, N. Souami, D. Sahel, I. Toumert, Characterization of mesoporous carbon prepared from date stems by H_3PO_4 chemical activation, Appl. Surf. Sci., 280 (2013) 1–7.

[38] L.Y. Hsu, H.S. Teng, Influence of different chemical reagents on the preparation of activated carbons from bituminous coal, Fuel Process. Technol., 64 (2000) 155–166.

[39] N. Bouchenafa-Saıb, G. Grange, P. Verhasselt, F. Addou, V. Dubois, Effect of oxidant treatment of date pit active carbons used as Pd supports in catalytic hydrogenation of nitrobenzene, Appl. Catal., A, 286 (2005) 167–174.

[40] S. Bruauner, P.H. Emmett, E. Teller, Adsorption of gases in multimolecular layers, J. Am. Chem. Soc., 60 (1938) 309–319.

[41] M.M. Dubinin, A.V. Astakhov, Development of the concept of the volume filling of micropores for vapors and gases adsorption on microporous adsorbents, Izv. AN SSSR, Ser. Khim, 20 (1971) 3–7.

[42] B. Cheknane, O. Bouras, M. Baudu, J.P. Basly, A. Cherguielaine, Granular inorgano-organo pillared clays (GIOCs): preparation by wet granulation, characterization and application to the removal of a Basic dye (BY28) from aqueous solutions, Chem. Eng. J., 158 (2010) 528–534.